Tetrahedral silicon-centered imidazolyl derivatives: Promising candidates for OLEDs and fluorescence response of Ag (I) ion

Dengxu Wang, Yuzhong Niu, Yike Wang, Jianjun Han, Shengyu Feng*

Key Laboratory of Special Functional Aggregated Materials of Ministry of Education; School of Chemistry and Chemical Engineering, Shandong University, Jinan 250100, PR China

ARTICLE INFO

ABSTRACT

A series of novel tetrahedral silicon-centered imidazolyl derivatives, Bis(4-(imidazol-1-yl)phenyl)dimethylsilane (**1**), Tri(4-(imidazol-1-yl)phenyl)methyl silane (**2**), Bis(4-(imidazol-1-yl)phenyl)diphenylsilane (**3**), Tri(4-(imidazol-1-yl)phenyl)phenylsilane (**4**), [Bis(4-(imidazol-1-yl)phenyl)](4-bromophenyl)phenylsilane (**5**) and [Tri(4-(imidazol-1-yl)phenyl)](4-bromophenyl)silane (**6**) have been synthesized and characterized by FTIR, ^{1}H NMR, ^{13}C NMR and mass spectroscopy. They all display high thermal stability, are fluorescent with emission in the region of violet to blue, and possess large HOMO-LUMO energy gaps ranging from 4.9585 to 5.1879 eV, which could be potentially used as blue emitters or hole blocking materials in OLEDs. Moreover, the metal ion titrations based on Ag (I) and compounds **1**–**4** reveal that these ligands show distinguishable fluorescence response with increasing of Ag (I) ions.

© 2010 Elsevier B.V. All rights reserved.

1. Introduction

Luminescent materials based on tetrahedral silicon-centered organic small molecules have attracted extensive interests due to their potential applications in sensor technologies as well as organic light emitting devices (OLEDs) [1–11]. These silicon-based molecules have many advantages such as well-defined structures and high color purity as evidenced by narrow emissions with high photoluminescence quantum yields in solid films [12,13]. They have been demonstrated to have good film-forming properties with high glass-transition temperature (T_g) and high thermal stability, and can be used to develop non-aggregating amorphous electroluminescent devices [14–17]. A large number of silicon-cored molecules have been designed, synthesized and used as highly efficient blue electroluminescent devices [18–21]. Furthermore, these tetrahedral shaped molecules based on silane core have been proved to be fascinating building blocks for constructing 3D porous metal-organic frameworks (MOFs) [22–25].

Imidazole-containing compounds have been widely investigated for their potential applications in OLEDs and coordination chemistry [26–30]. In the past decades, imidazole and its derivatives have been successfully applied as electron transport materials in OLEDs or as sensors for metal ions by themselves or by binding to the main or side chains in polymers [31–33]. Furthermore, it has been demonstrated that these molecules can be used as efficient ligands to assemble coordination polymers with intriguing molecular topologies and can be potentially used in the fields of photoelectronic devices, molecular recognition, ion changes and luminescent sensors [34–36].

Motivated by the demand for OLEDs and functional MOFs, we combined imidazolyl moiety and silicon core together derived from the precursors, $R_nSi(p\text{-}C_6H_4Br)_{4-n}$. In our previous work, we have designed and synthesized a silicon-centered imidazole compound, $Me_2Si(p\text{-}C_6H_4\text{-}imdazol\text{-}1\text{-}yl)_2$ (**1**). Based on this silicon-linked ligand, a novel three-dimensional (3D) MOF with a unique 3D-braided framework has been achieved. The research on the porous properties of the MOF showed that it possessed selective anion exchange property [37]. As an extension of our previous investigation, a series of novel tetrahedral silicon-centered imidazolyl compounds, $MeSi(p\text{-}C_6H_4\text{-}imidazol\text{-}1\text{-}yl)_3$ (**2**), $Ph_2Si(p\text{-}C_6H_4\text{-}imdazol\text{-}1\text{-}yl)_2$ (**3**), $PhSi(p\text{-}C_6H_4\text{-}imidazol\text{-}1\text{-}yl)_3$ (**4**), $Ph(p\text{-}C_6H_4Br)Si(p\text{-}C_6H_4\text{-}imidazol\text{-}1\text{-}yl)_2$ (**5**) and $(p\text{-}C_6H_4Br)Si(p\text{-}C_6H_4\text{-}imdazol\text{-}1\text{-}yl)_3$ (**6**) were synthesized via mono-lithiation, Si–C coupling reaction and Ullmann condensation reaction. Luminescent properties investigation revealed that all of them exhibited a strong and narrow emission in the region of violet to blue and could be potentially used as blue emitters in OLEDs. The interactions between these compounds and Ag (I) ion were also discussed.

2. Results and discussion

2.1. Synthesis and crystal structure

The tetrahedral silicon-centered imidazolyl derivatives, **1**–**6** were synthesized in a similar procedure according to the synthetic routes described in Scheme 1. Firstly, a reaction between 1,4-dibormobenzene and 1 equivalent *n*-BuLi afforded mono-lithiated

1,4-dibormobenzene, which reacted with the appropriate chloro-substituted silanes to give a series of bromophenyl-containing silanes, **8**–**12** [38–40]. Then, the tetrahedral silicon-centered imidazolyl derivatives, **1**–**6** were achieved using modified Ullmann condensation method under copper-catalyzed system by the reactions of **8**–**12** and imidazole. In our previous work, compound **1** has been synthesized using CuI as a catalyst and *N, N*-dimethyl-glycine as a promoter at 110 °C for 48 h in DMSO (Method B) in
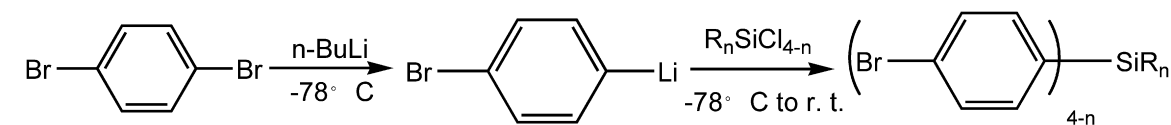
8: R=Me, n=2;   **9:** R=Me, n=1;
10: R=Ph, n=2; **11:** R=Ph, n=1;
12: n=0;   **13:** R=Me, n=3.
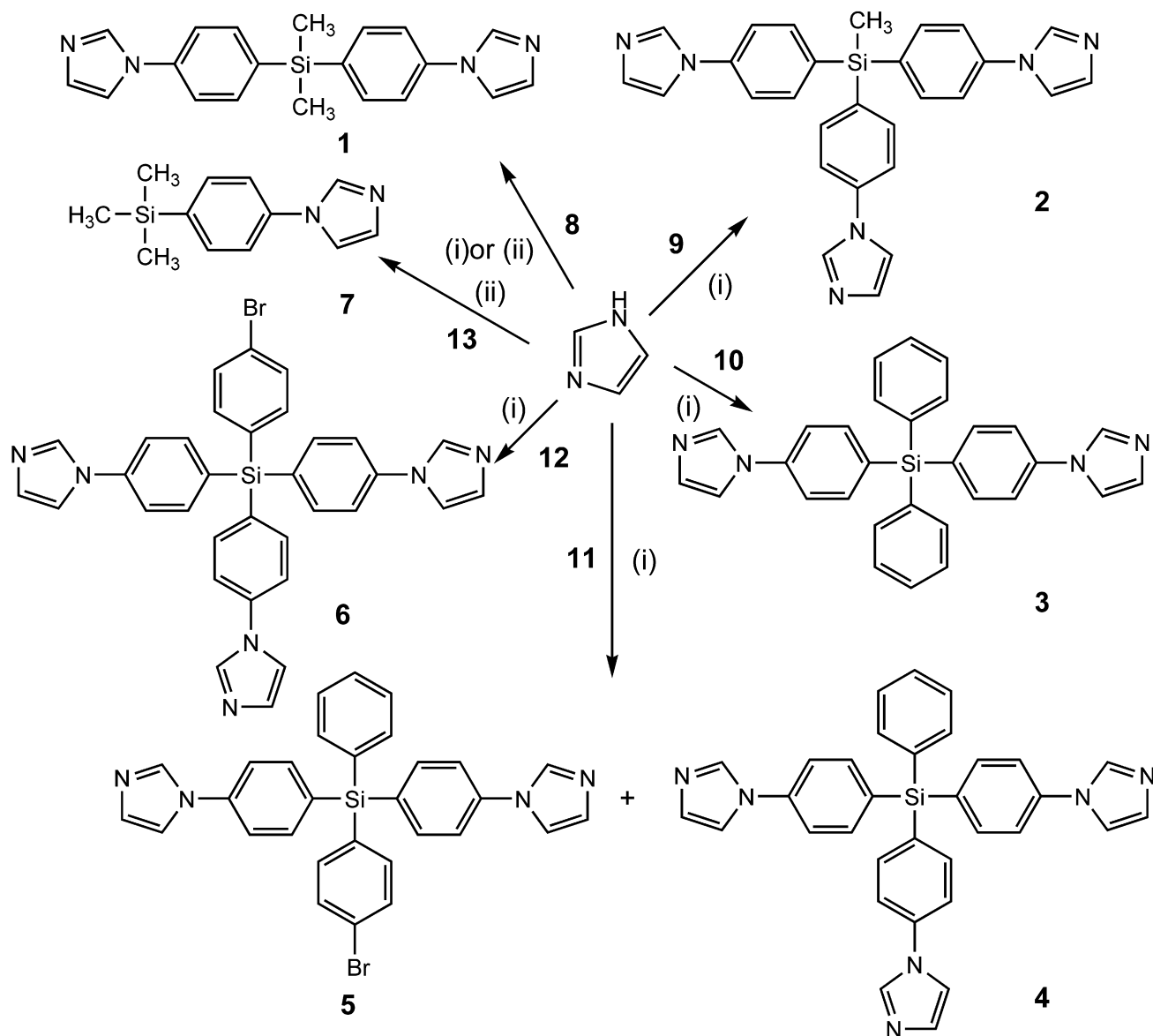
Scheme 1. Synthesis routes of bromophenyl-containing silanes **8**–**13** and imidazolyl derivatives **1**–**7**. (i) CuSO$_4$, K$_2$CO$_3$, 180 °C, 24 h; (ii) CuI/*N, N*-dimethylglycine, K$_2$CO$_3$, DMSO, 110 °C, 48 h.

a good yield [37]. However, Method B did not work when it was used to synthesize the imidazolyl derivatives 2–6 despite the raw materials 8–12 owning similar structures. The main by-product obtained was testified to be 1-phenylimidazole, as evidenced by ^{1}H NMR and mass spectrometry (Fig. S1). It is proposed that in this reaction N, N-dimethylglycine acts as a Lewis acid, which could induce Si–Ph rupture. This can be proved by the comparable yield of the by-product with the starting materials, although N, N-dimethylglycine was able to promote the formation of Ullmann-type C–N bond [41]. In order to achieve the target compounds, the reaction temperature was raised to 180 °C using $CuSO_4$ instead of CuI/N, N-dimethylglycine as the catalyst for 24 h without solvent in the Teflon autoclave (Method A). The first synthesis of compound 1 by using Method A indicated that Ullmann condensation reaction could also proceed well in this case. Compared to the synthesis of 1 in Method B, the yield was slightly lower in Method A. Furthermore, the imidazole-containing silanes, 2–6 were also synthesized successfully by using Method A. Compounds 2 and 3 were separated in a moderate yield of ~25%. Compounds 4 and 5 were isolated as two main products from the same starting material, tri(4-bromophenyl)phenylsilane (11) in the yields of 14.9% and 11.0%, respectively. The synthesis of compound 6 was more challenging because of the possibility of the formation of mono-, di-, tri-, or tetra-substituted product as well as the existence of unreacted starting materials and other by-products in the reaction mixture, which made the separation and purification difficult. In addition, the similar polarity of the substituted products further complicated the product separation. Initially the tetra-substituted product, tetra(4-(imidazol-1-yl)phenyl)silane was our target product. However, the tri-substituted product, 6 was isolated in 10% yield as the main product. We attempted to raise the reaction temperature to 200 °C or prolonged the reaction time to 48 h. It was found that there was no obvious enhancement for the formation of 6 or the tetra-substituted product but more by-products, mainly 1-phenyl-imidazole were observed. This may be attributed to the great steric hindrance of tetra(4-bromophenyl)silane (12). On the other hand, the formation of Ullmann-type C–N bond may accompany with the cleavage of Si–Ph bond under this high reaction temperature. In addition, we have also synthesized the mono-substituted product, (4-(imidazol-1-yl)phenyl)trimethylsilane (7) and the synthesis procedure was similar to that of compound 1 (Scheme 1). It was demonstrated that compound 7 can be achieved successfully according to Method B in a high yield. Compounds 1–7 were fully characterized by FTIR, ^{1}H NMR, ^{13}C NMR and mass spectroscopy.

In our previous report [37], single crystal X-ray diffraction analyses show that the molecule of 1 has a tetrahedral structure around silicon atom with the average dihedral angel of 41.024° between imidazole ring and benzene ring, which indicates that the degree of conjugation throughout the molecule is relatively small. It is noteworthy that the adjacent molecules stack along ab plane with intermolecular π–π interactions between imidazole rings and benzene rings with the shortest atomic contact distance being ~2.9 Å (Fig. 1).

2.2. Thermal properties

The thermal properties of compounds 1–6 were firstly determined by the thermogravimetric analysis (TGA) with a heating rate of 10 °C/min under nitrogen. The results show that 2–6 are stable up to over 300 °C while 1 decomposes at about 250 °C, which may be owing to the lower thermal stability of two Si–CH_3 groups in 1 compared to other compounds with more Si–Ph groups (Fig. S3). Compounds 1 and 2 show a small percentage of weight loss below 200 °C, which can be attributed to the loss of solvent molecules embedded in the compounds. The examinations by differential
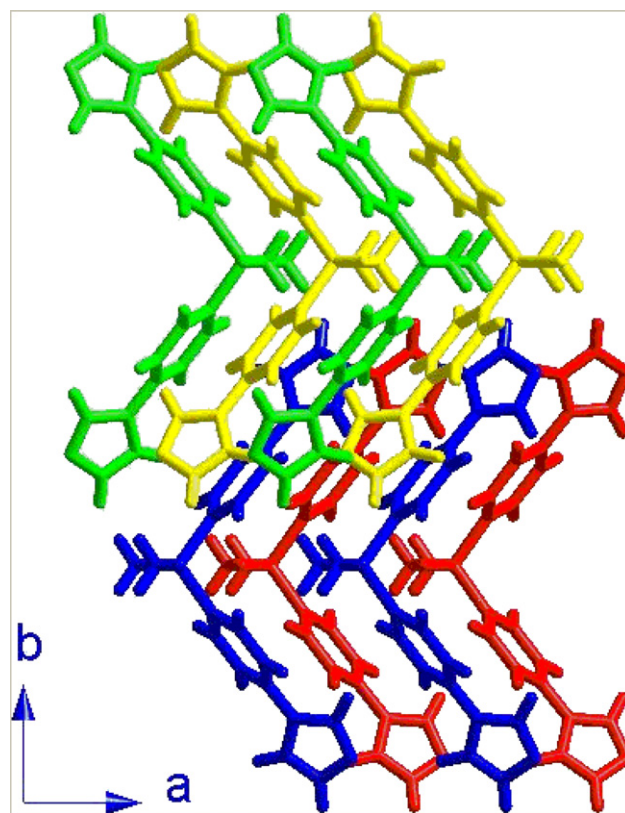

Fig. 1. Packing diagram showing the π–π interactions between adjacent molecules of 1. Water molecules are omitted for clarify.

scanning calorimetry (DSC) show that neither obvious melting points (T_m) nor glass-transition temperatures (T_g) were detected for compounds 4, 5 and 6 while T_m of compounds 1 and 2 were observed at 174 °C and 221 °C, respectively, and the crystalline temperature (T_c) and T_m of compound 3 were observed at 58 °C and 169 °C, respectively (Fig. S2).

2.3. Photophysical properties and molecular orbital calculations

To investigate the possibilities of 1–6 applying in OLEDs, UV–vis and luminescent spectra were measured. Fig. 2 shows the UV–vis absorption spectra of 1–6 in CH_2Cl_2 solution. As expected, 1–6 all
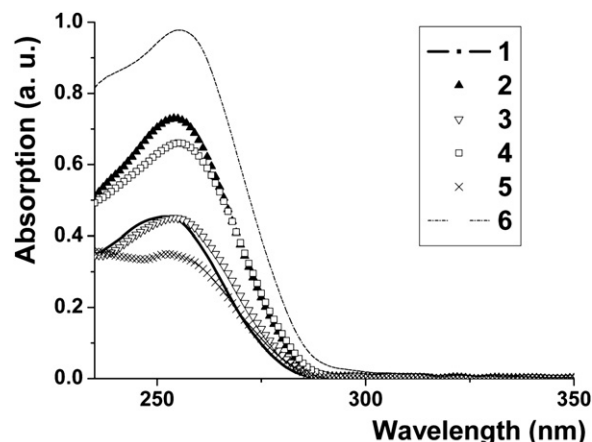

Fig. 2. UV–vis spectra of 1–6 in CH_2Cl_2 solution (1×10^{-5} M).
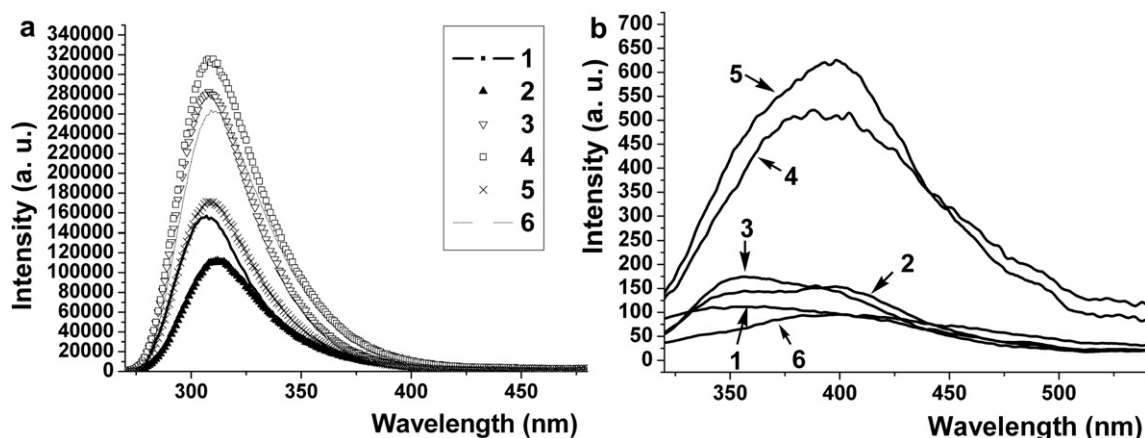
Fig. 3. Emission spectra of **1**–**6** (a) in CH_2Cl_2 solution (1×10^{-5} M, $\lambda_{ex} = 250$ nm); (b) in the solid state ($\lambda_{ex} = 290$ nm).

exhibit one similar intense absorption band with λ_{max} at ~255 nm, which can be attributed to the π–π^* transitions involving the phenyl and imidazole groups. Furthermore, **1**–**6** are all luminescent and emit a violet–blue color in solution and in the solid state when irradiated by UV light. Similar to UV–vis spectra, **1**–**6** display analogic fluorescence spectra with the maximum emission wavelength at ~310 nm in CH_2Cl_2 solution (Fig. 3a). In the solid state, **1**–**6** display a broad emission from violet to blue region with the emission wavelength maximum ranging from 356 nm (**3**) to 399 nm (**6**) (Fig. 3b and Table 1). Moreover, the emission spectra in the solid state for **1**–**6** are considerably red-shifted compared with that in solution, which is obviously caused by extensive intermolecular interactions, such as π–π stacking interactions as displayed by compound **1** (Fig. 1). In addition, compounds **4** and **5** exhibit stronger emission than other compounds, indicating that in **4** and **5** stronger intermolecular interactions may exist. Despite these imidazolyl derivatives showing strong and narrow emissions in the region of violet to blue, the emission quantum efficiencies are low and vary between 0.051 (**6**) and 0.12 (**5**).

The low luminescence quantum efficiencies may be attributed to two reasons: (i) low π-conjugated degree of aromatic rings in these compounds. For example, in the crystal structure of compound **1**, the average dihedral angel between imidazole ring and benzene ring is 41.024°, which is a convincing evidence of the small conjugation degree throughout the molecule. (ii) The limited $d\pi$–$p\pi$ conjugation effect of the silicon core. Silicon atom has empty 3d orbitals which can conjugate with adjacent atom or π-conjugated system to form $d\pi$–$p\pi$ conjugation. However, this conjugation action is generally limited. To investigate how silicon cores affect the luminescent properties,

UV–vis and luminescent spectra of the mono-substituted imidazole derivative, compound **7** were also measured. The results revealed that compound **7** displayed a similar UV–vis absorption and emission spectra to that of compound **1**–**6**, which were distinctly due to imidazole and phenyl groups in the compound **7** (Fig. S6 and S7). Therefore, silicon core had weak effect on the π-conjugated system, which led to the low conjugation degree of the whole compound.

Compared with previous reports on luminescent organic small molecules or polymers used as OLEDs [42–44], the UV–vis spectra and emission spectra of **1**–**6** are all blue-shifted. The reasons for this might be that, imidazole as a functional group in these molecules obviously owns lower π-conjugated system with lower electron density, and hence makes limited contributions to luminescent properties compared with other functional groups, such as 2,2′-dipyridylamine, carbazole, condensed nucleus and so on [5–7]. Moreover, as mentioned above, the $d\pi$–$p\pi$ conjugation action of silicon atom is generally limited and silicon atom is more inclined to interrupt the π-conjugated system and disturb the coplanarity of the π-conjugated compounds. However, the incorporation of silicon atom to these compounds can improve their color purity due to the narrow emission, which makes them promising candidates for blue emitters in OLEDs displays.

In order to gain a deeper insight into their electronic and luminescent properties, molecular orbital calculations have been performed at the level of B3LYP/6-31G(d) using the Gaussian 03 suite of programs [45]. The contour plots of the HOMO and LUMO frontier molecular orbitals and HOMO, LUMO energies and energy gaps of **1**–**6** are shown in Fig. 4 (**2**, **4** and **6**) and Fig. S8 (**1**, **3** and **5**). As can be

Table 1
UV–vis and Luminescent data for compounds **1**–**6**.

Compound	UV–vis absorption (nm)	ε (M^{-1} cm^{-1})	Excitation (nm)	Emission (nm)	Quantum yield	Conditions (298 K)
1	252	4.54×10^4	256	309	0.094	CH_2Cl_2
			235, 330	395		Solid slate
2	254	7.29×10^4	250	315	0.062	CH_2Cl_2
			244, 328	398		Solid slate
3	254	4.51×10^4	255	308	0.093	CH_2Cl_2
			244, 320	356		Solid slate
4	255	6.60×10^4	255	312	0.073	CH_2Cl_2
			315	388		Solid slate
5	252	3.50×10^4	251	307	0.12	CH_2Cl_2
			245, 330	398		Solid slate
6	256	9.78×10^4	255	313	0.051	CH_2Cl_2
			243, 334	399		Solid slate

$E_H=-6.2832$ eV $E_H=-6.2805$ eV $E_H=-6.3458$ eV

HOMO

$E_L=-1.1342$ eV $E_L=-1.2757$ eV $E_L=-1.3873$ eV

LUMO

$E_{H-L\ gap}=5.1490$ eV $E_{H-L\ gap}=5.0048$ eV $E_{H-L\ gap}=4.9585$ eV
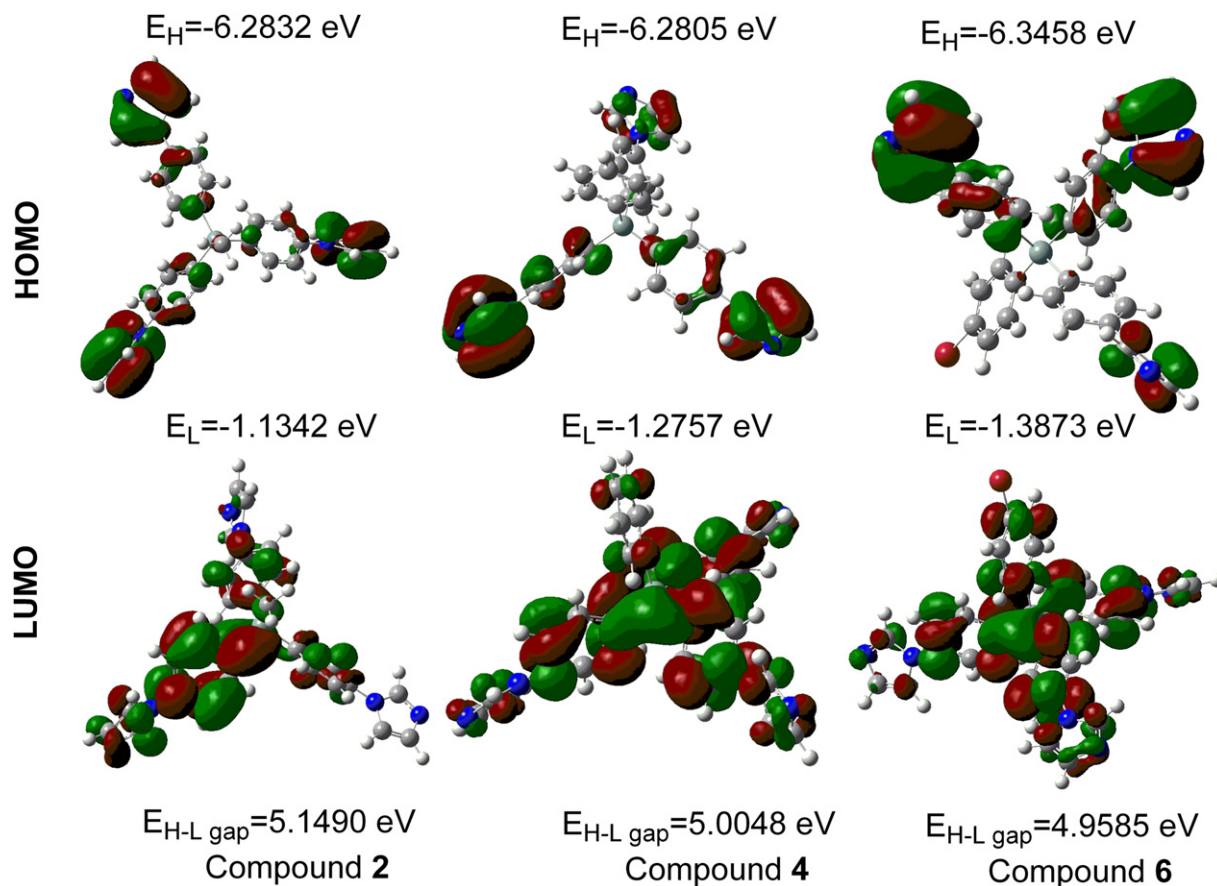Compound **2**   Compound **4**   Compound **6**

Fig. 4. HOMO and LUMO energies, energy gaps and orbital diagrams of **2**, **4** and **6**.

seen from Fig. 4 and Fig. S8, the HOMOs of these compounds are similar, with dominating contributions from the orbitals of the imidazolyl groups, while LOMOs involves contributions from the entire molecules. The bromo-substituted groups in **5** and **6** didn't have contribution to the HOMO or LUMO orbitals. The results also indicated that the tetrahedral silicon core does not have significant effect on the electronic properties of **1**–**6**, which is consistent with previous reports [6,7]. It is noteworthy that these compounds all have a deep energy gap with the range from 4.9585 eV (**6**) to 5.1879 eV (**1**). The deep HOMO level for this series of molecules is a strong indication that they may be potentially useful candidates as efficient hole blocking materials in OLEDs [7,46].

2.4. Interactions with Ag (I) ion

In recent years much attention has been paid on the negative impact of silver ions on the environment and organisms due to the extensive applications and broad prospects of silver in the electronic industry and optical fields. It has been demonstrated that fluorescence spectroscopy is an effective method to detect trace amounts of silver ions in environmental and biological system because of its high sensitivity and facile operation [47–49]. So here we examined the impact of Ag(I) ion binding on the fluorescence of compounds **1**–**4** using AgClO$_4$ as the titrant.

The UV–vis spectroscopic properties of compounds **1**–**4** interacting with Ag (I) ion in CH$_2$Cl$_2$ solution were firstly evaluated. With the increasing of silver ions (0–2 equiv for **1** and **3**, 0–3 equiv for **2** and **4**), the maximum absorptions of compounds **1**, **2** and **4** show a slight blue-shift with no intensity decreasing, while that of compound **3** also displays a small blue-shift but

intensity gradually decreasing (Fig. S9). The fluorescent titration results reveal that all the compounds show a fluorescent quenching response and a slight blue-shift with the addition of AgClO$_4$ (Fig. 5). Similar to other N-donor ligands, the fluorescent changes for all the compounds are completed when adding about 1 equivalent AgClO$_4$, although compounds **2** and **4** have a larger number of potential sites than **1** and **3**. This suggests that the full fluorescent quenching effect of Ag (I) ion can be viewed without saturation of all of the coordination sites on the ligand or that Ag (I) displays multiple coordination modes and a single Ag(I) ion may bind to several ligands in solution. For compound **1**, when the [Ag]/[Lig] ratio reached 1:1, the fluorescence intensity dropped 50% (Fig. 6). Unlike in solution, the silver complex in the solid state with the [Ag]/[Lig] ratio of 1:1 displayed a dramatic decrease with the overall reduction of 93% [37]. It is proposed that Ag(I) ion has a much larger heavy-atom effect on the fluorescence of **1** in the solid state than in solution. Similar to compound **1**, the fluorescent intensity of compounds **2**, **3** and **4** also decreased but showed greater fluorescent reduction. As the end of the fluorescent quenching, the overall reduction is 75% for **2**, 97% for **3** and 95% for **4** (Fig. 6). The evaluation over various imidazolyl derivatives, **1**–**4**, reveals that the fluorophore is responsive to Ag (I) with better response of compounds **3** and **4**. In addition, as a typical compound, binding analysis using the method of continuous variations (Job's plot) established a 1:1 stoichiometry for the **4**-Ag$^+$ complex. Following the Benesi- Hildebrand-type analysis, the binding constant K_a value was determined to be 1.37 × 10^5 (Supporting information), which proved that strong binding force existed between **4** and Ag(I) ion in CH$_2$Cl$_2$ solution. Theses results speculate that the potential show distinct luminescence responses
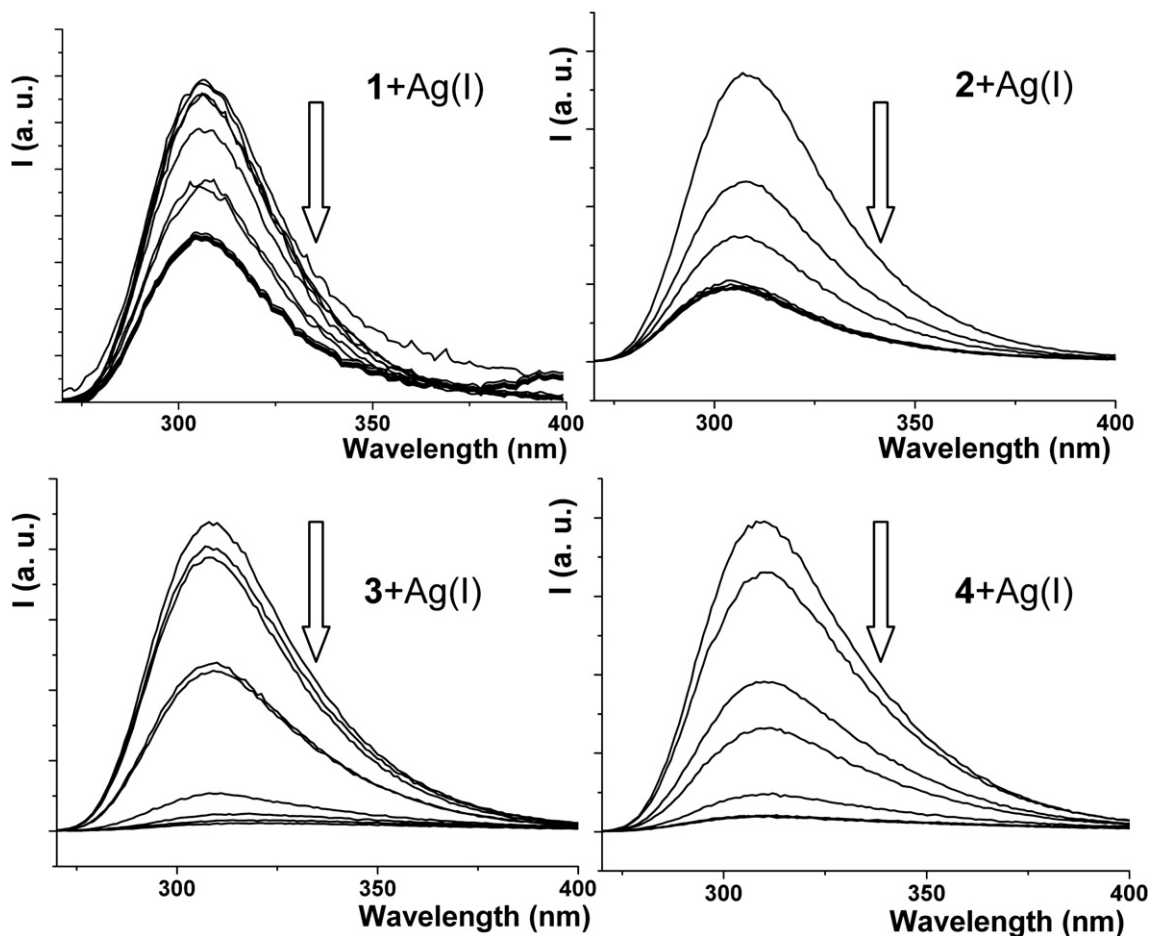
Fig. 5. Fluorescent titration results of compounds **1–4** in CH_2Cl_2 solution with $AgClO_4$ at 1×10^{-5} M ($\lambda_{ex} = 250$ nm for all the compounds).
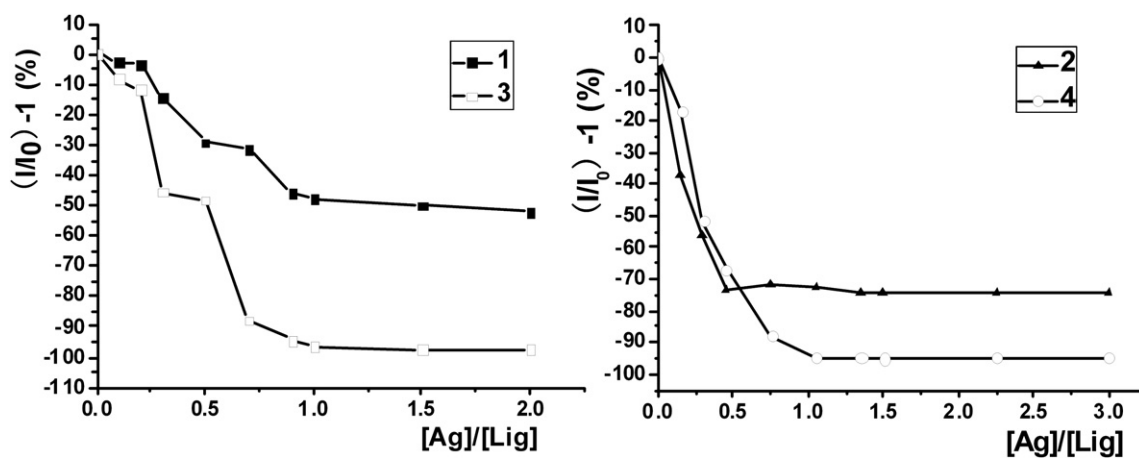

Fig. 6. The reduction of fluorescence intensities of **1–4** in CH_2Cl_2 solution upon addition of Ag (I) ($\lambda_{ex} = 250$ nm for all the compounds).

on binding to Ag (I) center when these imidazolyl derivatives act as ligands in coordination chemistry.

3. Conclusions

In summary, a series of novel imidazolyl functionalized tetrahedral silicon-centered molecules have been synthesized and characterized. TGA measurements revealed that all the compounds have high thermal stability. The luminescent properties and molecular orbital calculation indicated that these organic small molecules could be potentially applied not only as blue emitter but also hole blocking materials in OLEDs. According to the investigation of metal ion titration, compounds **1–4** showed distinct fluorescence response for Ag(I) ion. Further research will focus on the construction of functional MOFs based on these imidazole-containing building blocks and examining their numerous potential properties such as molecular recognition, ion exchange etc.

4. Experimental

4.1. General

Unless otherwise noted, all reagents were obtained from commercial suppliers and used without further purification. Dimethyl sulfoxide (DMSO) was first dried over CaH_2 at 80 °C for 1 day and distilled under vacuum pressure. Then DMSO was stored with 4 Å molecule sieves prior to use. Ether was dried by distillation from the sodium ketyl of benzophenone. FTIR were recorded on a Bruker Tensor27 spectrophotometer, the spectrometers were acquired in the frequency range 4000–400 cm^{-1} at a resolution of 4 cm^{-1} with a total of 32 scans. ^1H NMR and ^{13}C NMR spectra were measured on a Bruker AVANCE-300 or 400 NMR Spectrometer. High-resolution mass spectra were obtained using positive mode on Aglient Technologies 6510 Q-TOF LC-MS. Elemental analyses (C, H, N) were obtained on a Perkin–Elmer 240 elemental analyzer. TGA was performed with a MettlerToledo SDTA-854 TGA system in nitrogen at a heating rate of 10 °C/min. DSC measurements were carried out in MettlerToledo DSC822 series ramping from 10 to 300 °C at the rate of 10 °C/min in a steady flow of nitrogen (20 ml/min). The fluorescence spectra were determined with ISS K2-Digital spectrophotometer: excitation slit width = 10 nm, emission slit width = 3 nm. Luminescence quantum yields were measured using quinine sulfate in 0.1 N H_2SO_4 (Φ = 54.6%) as reference. The quantum yields were calculated according to the procedures described elsewhere [50,51].

4.2. Synthesis of bis(4-bromophenyl)dimethylsilane (8)

1,4-dibromobenzene (2.36 g, 10 mmol) was dissolved in dry Et_2O (100 mL) and cooled to −78 °C under argon. n-BuLi (2.5 M in hexanes, 4 mL, 10 mmol) was added into this solution dropwise and stirred for another 1 h at −78 °C. Dichlorodimethylsilane (0.64 g, 5 mmol) was then added dropwise at this temperature. After the end of the addition, the reaction mixture was slowly raised to room temperature and stirred overnight. Then the reaction was quenched by 30 mL H_2O and the organic layer was separated. The water layer was washed by 30 mL Et_2O twice. The organic layers were combined, washed by brine, dried over anhydrous $MgSO_4$ and then filtered. Removal of the solvents under vacuum gave the crude product, which was recrystallized from hexane to obtain 8. Yield: 78.3%. IR (KBr pellet cm^{-1}): 3031, 3012, 2961, 1566, 1477, 1375, 1254, 1105, 1066, 1007, 832, 812, 723, 660. ^1H NMR (300 MHz, CDCl$_3$) δ 0.53 (s, 6H), 7.34 (d, 4H, J = 8.1 Hz), 7.49 (d, 4H, J = 8.1 Hz).

4.3. Synthesis of Tri(4-bromophenyl)methylsilane (9)

The preparation procedure of 9 was analogous to that described for 8. Yield: 83.5%. IR (KBr pellet cm^{-1}): 3074, 3006, 2962, 1568, 1549, 1476, 1376, 1252, 1110, 1066, 1009, 809, 781, 721. ^1H NMR (300 MHz, CDCl$_3$) δ 0.79 (s, 3H), 7.30 (d, 6H, J = 8.4 Hz), 7.50 (d, 6H, J = 8.1 Hz).

4.4. Synthesis of bis(4-bromophenyl)diphenylsilane (10)

The preparation procedure of 10 was similar to that of 8 except that the product was recrystallized from CHCl$_3$–EtOH. Yield: 65.9%. IR (KBr pellet cm^{-1}): 3065, 3024, 1645, 1568, 1477, 1377, 1111, 1063, 1008, 810, 728, 698. ^1H NMR (300 MHz, CDCl$_3$) δ 7.36–7.59 (m, 18H).

4.5. Synthesis of tri(4-bromophenyl)phenylsilane (11)

The preparation procedure of 11 was similar to that of 10. Yield: 55.6%. IR (KBr pellet cm^{-1}): 3065, 3024, 1645, 1568, 1477, 1377, 1111, 1063, 1008, 810, 728, 698. ^1H NMR (300 MHz, CDCl$_3$) δ 7.35–7.54 (m, 17H).

4.6. Synthesis of tetra(4-bromophenyl)silane (12)

The preparation procedure of 12 was similar to that of 10. Yield: 52.6%. IR (KBr pellet cm^{-1}): 3075, 3010, 1617, 1458, 1376, 1058, 995, 803. ^1H NMR (300 MHz, CDCl$_3$) δ 7.35 (d, 8H, J = 8.1 Hz), 7.52 (d, 8H, J = 8.4 Hz).

4.7. Synthesis of (4-bromophenyl)trimethylsilane (13)

The preparation procedure of 13 was similar to that of 8 except that the product was distillated under vacuum pressure with b. p. 110–114 °C/6 mmHg. IR (KBr pellet cm^{-1}): 3070, 3034, 3014, 2955, 2896, 1573, 1479, 1375, 1248, 1106, 1066, 1011, 830, 812, 752, 660. ^1H NMR (300 MHz, CDCl$_3$) δ 0.25 (s, 9H), 7.36 (d, 2H, J = 8.1 Hz), 7.47 (d, 2H, J = 8.1 Hz).

4.8. Synthesis of bis(4-(imidazol-1-yl)phenyl)dimethylsilane (1)

4.8.1. Method A
Bis(4-bromophenyl) dimethylsilane (1.85 g, 5 mmol), imidazole (0.85 g, 12.5 mmol), K_2CO_3 (2.76 g, 20 mmol) and $CuSO_4$ (0.016 g, 0.1 mmol) were heated at 180 °C for 24 h in a Teflon autoclave under argon. After cooling to ambient temperature, the mixture was dissolved in 50 mL CHCl$_3$ and washed with water. The water layer was separated and extracted with CHCl$_3$ (3 × 30 mL). The combined organic layers were washed with water (3 × 30 mL), dried over anhydrous $MgSO_4$ and filtered. The solvents were evaporated under reduced pressure and a white solid was obtained by column chromatography (CH$_2$Cl$_2$/MeOH as eluent). Yield: 40.1%.

4.8.2. Method B
A four-bottled flask was charged with bis(4-bromophenyl) dimethylsilane (1.85 g, 5 mmol), imidazole (0.85 g, 12.5 mmol), K_2CO_3 (2.76 g, 20 mmol), CuI (0.19 g, 1 mmol) and N, N-dimethlyglycine (0.20 g, 2 mmol) and backfilled with argon, followed by addition of 25 ml DMSO. Then the mixture was heated at 110 °C for 48 h before it was partitioned between water and ethyl acetate. The organic layer was separated, and the aqueous layers were washed with ethyl acetate. The combined organic layers were washed with brine, dried with $MgSO_4$ and concentrated in vacuum. A white powder was obtained by column chromatography (CH$_2$Cl$_2$/MeOH as eluent). Yield: 46.5%. IR (KBr pellet cm^{-1}): 3112, 3031, 2959, 1596, 1511, 1399, 1373, 1303, 1251, 1097, 1056, 959, 903, 817, 739, 659, 538. ^1H NMR (400 MHz, DMSO) δ 8.26 (s, 2H), 7.75 (s, 2H), 7.65 (s, 8H), 7.11 (s, 2H), 0.60 (s, 6H). ^{13}C NMR (400 MHz, DMSO): δ 138.2, 136.6, 136.0, 135.9, 130.4, 120.3, 118.4, −2.3. HRMS (FAB) calcd for $C_{20}H_{20}N_4Si$ (MH$^+$): 345.1530, found 345.1527. Anal. Calcd for $C_{20}H_{20}N_4Si$/CH$_2$Cl$_2$: C, 64.02; H, 5.63; N, 14.22. Found: C, 64.64; H, 5.61; N, 14.76.

4.9. Synthesis of tri(4-(imidazol-1-yl)phenyl)methylsilane (2)

A Teflon autoclave was charged with tris(4-bromophenyl) methylsilane (1.28 g, 2.5 mmol), imidazole (1.02 g, 15 mmol), K_2CO_3 (1.38 g, 10 mmol) and $CuSO_4$ (0.016 g, 0.1 mmol) and backfilled with argon. The mixture was heated at 180 °C for 24 h. The treatment procedure for product was analogous to that described for 1 in Method A and a white solid was obtained. Yield: 25.3%. IR (KBr pellet cm^{-1}): 3107, 3031, 2955, 2894, 1595, 1512, 1402, 1304, 1253, 1191, 1098, 1054, 958, 903, 823, 791, 739, 656, 537. ^1H NMR (300 MHz, DMSO) δ 8.32 (s, 3H), 7.83 (s, 3H), 7.73 (d, 6H, J = 8.4 Hz), 7.63 (d, 6H, J = 8.4 Hz), 7.13 (s, 3H), 0.94 (s, 3H). ^{13}C NMR (300 MHz,

DMSO) δ 140.27, 138.66, 137.77, 135.79, 132.25, 122.17, 120.10, −1.71. HRMS (FAB) calcd for $C_{28}H_{24}N_6Si$ (MH^+): 473.1904, found 473.1903. Anal. Calcd for $C_{28}H_{24}N_6Si$: C, 71.16; H, 5.12; N, 17.78. Found: C, 71.02; H, 5.12; N, 17.13.

4.10. Synthesis of bis(4-(imidazol-1-yl)phenyl)diphenylsilane (3)

A Teflon autoclave was charged with bis(4-bromophenyl)phenylsilane (1.23 g, 2.5 mmol), imidazole (0.68 g, 10 mmol), K_2CO_3 (1.03 g, 7.5 mmol) and $CuSO_4$ (0.008 g, 0.05 mmol) and backfilled with argon. The mixture was heated at 180 °C for 24 h. The treatment procedure for product was analogous to that described for 1 in Method A and a colorless crystal was obtained. Yield: 25.6%. IR (KBr pellet cm^{-1}): 3109, 3062, 3045, 3024, 1595, 1511, 1426, 1402, 1302, 1249, 1190, 1111, 1098, 1052, 958, 901, 818, 792, 740, 656, 537. ^{1}H NMR (300 MHz, DMSO) δ 8.33 (s, 2H), 7.80 (s, 3H), 7.76 (d, 4H, J = 8.4 Hz), 7.62 (d, 4H, J = 8.4 Hz), 7.46−7.53 (m, 10H), 7.15 (s, 2H). ^{13}C NMR (300 MHz, DMSO) δ 140.42, 139.57, 138.00, 135.08, 133.90, 132.36, 130.55, 122.27. HRMS (FAB) calcd for $C_{30}H_{24}N_4Si$ (MH^+): 469.1843, found 469.1823. Anal. Calcd for $C_{30}H_{24}N_4Si$: C, 76.89; H, 5.16; N, 11.96. Found: C, 75.60; H, 5.10; N, 11.73.

4.11. Synthesis of tri(4-(imidazol-1-yl)phenyl)phenylsilane (4) and [bis(4-(imidazol-1-yl)phenyl)] (4-bromophenyl)phenylsilane (5)

A Teflon autoclave was charged with tris(4-bromophenyl)phenylsilane (1.43 g, 2.5 mmol), imidazole (1.02 g, 15 mmol), K_2CO_3 (1.38 g, 10 mmol) and $CuSO_4$ (0.016 g, 0.1 mmol) and backfilled with argon. The mixture was heated at 180 °C for 24 h. The treatment procedure for product was analogous to that described for 1 in Method A and two products were obtained. 4 as a white solid was afforded by column chromatography with CH_2Cl_2/MeOH (25:1) as eluent (R_f = 0.2). Yield: 14.9%. IR (KBr pellet cm^{-1}): 3109, 3062, 3027, 1595, 1511, 1428, 1403, 1303, 1249, 1192, 1098, 1053, 959, 902, 819, 736, 670, 656, 552. ^{1}H NMR (300 MHz, DMSO) δ 8.33 (s, 3H), 7.46−7.53 (m, 18H), 7.14 (s, 3H). ^{13}C NMR (300 MHz, DMSO) δ 140.51, 139.59, 138.27, 138.01, 137.80, 134.79, 133.56, 132.33, 130.63, 122.32, 120.07. HRMS (FAB) calcd for $C_{33}H_{26}N_6Si$ (MH^+): 535.2061, found 535.2049. Anal. Calcd for $C_{33}H_{26}N_6Si$: C, 74.13; H, 4.90; N, 15.72. Found: C, 73.95; H, 4.58; N, 15.20. Meanwhile, 5 as a white solid was afforded by column chromatography with CH_2Cl_2/MeOH (15:1) as eluent (R_f = 0.3). Yield: 11.0%. IR (KBr pellet cm^{-1}): 3110, 3062, 3028, 1596, 1511, 1481, 1426, 1404, 1303, 1258, 1190, 1100, 1053, 959, 901, 813, 736, 699, 655, 547. ^{1}H NMR (400 MHz, DMSO) δ 8.30 (s, 2H), 7.45−7.49 (m, 3H), 7.50−7.55 (m, 5H), 7.60−7.63 (m, 4H), 7.73−7.76 (m, 5H), 7.13 (s, 2H). ^{13}C NMR (300 MHz, DMSO) δ 138.17, 137.61, 137.43, 137.21, 135.62, 135.42, 131.19, 131.03, 130.15, 129.98, 128.27, 128.18, 119.97, 117.69. HRMS (FAB) calcd for $C_{30}H_{23}N_4SiBr$ (MH^+): 547.0948, found 547.0927. Anal. Calcd for $C_{30}H_{23}N_4SiBr$: C, 65.81; H, 4.23; N, 10.23. Found: C, 65.62; H, 4.30; N, 10.18.

4.12. Synthesis of [tri(4-(imidazol-1-yl)phenyl)](4-bromophenyl) silane (6)

A Teflon autoclave was charged with tetra(4-bromophenyl) silane (1.63 g, 2.5 mmol), imidazole (1.36 g, 20 mmol), K_2CO_3 (2.07 g, 15 mmol) and $CuSO_4$ (0.016 g, 0.1 mmol) and backfilled with argon. The mixture was heated at 180 °C for 24 h. The treatment procedure for product was analogous to that described for 1 in Method A and a yellow solid was afforded. Yield: 10.5%. IR (KBr pellet cm^{-1}): 3107, 3027, 1596, 1511, 1480, 1403, 1372, 1249, 1192, 1097, 1053, 958, 902, 816, 737, 655, 552. ^{1}H NMR (300 MHz, DMSO) δ 8.33 (s, 3H), 7.47−7.83 (m, 19H), 7.14 (s, 3H). ^{13}C NMR (DMSO) δ 140.52, 139.80, 138.92, 138.00, 137.79, 133.60, 132.33, 130.62, 123.69, 122.33, 120.07. HRMS (FAB) calcd for $C_{33}H_{25}N_6SiBr$ (MH^+):

613.1166, found 613.1152. Anal. Calcd for $C_{33}H_{25}N_6SiBr$: C, 64.60; H, 4.11; N, 13.70. Found: C, 64.58; H, 4.15; N, 13.60.

4.13. Synthesis of (4-(imidazol-1-yl)phenyl)trimethylsilane (7)

The synthesis and treatment procedures for 7 were similar to that described for 1 in Method B and a yellow solid was afforded. Yield: 56.8%. IR (KBr pellet cm^{-1}): 3114, 3026, 2956, 2895, 1600, 1513, 1486, 1402, 1365, 1302, 1251, 1122, 1093, 1056, 960, 903, 840, 817, 752, 657, 533. ^{1}H NMR (400 MHz, DMSO) δ 8.28 (s, 1H), 7.76 (s, 1H), 7.64 (s, 4H), 7.12 (s, 1H), 0.27 (s, 9H). ^{13}C NMR (400 MHz, DMSO): δ 138.9, 137.9, 136.0, 135.2, 130.4, 120.1, 118.4, −0.7. HRMS (FAB) calcd for $C_{12}H_{16}N_2Si$ (MH^+): 217.1156, found 217.1145. Anal. Calcd for $C_{12}H_{16}N_2Si$: C, 66.62; H, 7.45; N, 12.95. Found: C, 66.03; H, 7.38; N, 12.65.

4.14. Metal titration experiments

Compounds 1−4 in dichloromethane solution (1×10^{-3} M) and silver perchlorate in methanol solution (1×10^{-3} M) were firstly prepared. Then a series of Ag (I) and ligands in dichloromethane were prepared with the [Ag]/[Lig] ratio from 0 to 2.0 for compounds 1 and 3 and 0 to 3.0 for compounds 2 and 4, while maintaining the ligands concentration of 1×10^{-5} M. Then the emission spectrum was measured after 24 h and the excitation wavelength was employed at 250 nm for all the compounds.

Appendix. Supplementary materials

Characterization for the by-product obtained, ^{1}H NMR spectrum of compounds 1−7, TGA and DSC curves of compounds 1−6, excitation spectra of compounds 1−7 and emission spectra of compound 7 in solution and in the solid state, UV spectra of compound 7, molecular orbital calculation for compounds 1, 3 and 5, UV change results of compounds 1−4 in CH_2Cl_2 solution with $AgClO_4$ and binding analysis for Ag^+ with compound 4. Supplementary data associated with this article can be found, in the online version, at doi:10.1016/j.joranchem.2010.06.026.

References

[1] Y.N. Luponosov, S.A. Ponomarenko, N.M. Surin, O.V. Borshchev, E.A. Shumilkina, A.M. Muzafarov, Chem. Mater. 21 (2009) 447.
[2] H. Kai, J. Ohshita, S. Ohara, N. Nakayama, A. Kunai, I.-S. Lee, Y.-W. Kwak, J. Organomet. Chem. 693 (2008) 3490.
[3] Y.N. Luponosov, S.A. Ponomarenko, N.M. Surin, A.M. Muzafarov, Org. Lett. 10 (2008) 2753.
[4] T. Lee, I. Jung, K.H. Song, H. Lee, J. Choi, K. Lee, B.J. Lee, J.Y. Pak, C. Lee, S.O. Kang, J. Ko, Organometallics 23 (2004) 5280.
[5] J. Roncali, P. Leriche, A. Cravino, Adv. Mater. 19 (2007) 2045.
[6] D.-R. Bai, X.Y. Liu, S.N. Wang, Chem. Eur. J. 13 (2007) 5713.
[7] D.-R. Bai, S.N. Wang, Organometallics 23 (2004) 5958.
[8] M.-L. Hung, C.-W. Ko, T.-H. Liu, U. S. Patent 0 115 674 2006.
[9] K. Nii, U. S. Patent 0 135 167 2004.
[10] J. Ogasawara, S. Watanabe, U. S. Patent 0 214 572 2005.
[11] T. Igarashi, T. Taguchi, U. S. Patent 6 310 231 2001.
[12] Q. Shen, S.Y. Ye, G. Yu, P. Lu, Y.Q. Liu, Synth. Met 158 (2008) 1054.
[13] X.M. Liu, J. Xu, X. Lu, C. He, Org. Lett. 7 (2005) 2829.
[14] X.M. Liu, T. Lin, J. Huang, X.T. Hao, K.S. Ong, C. He, Macromolecules 38 (2005) 4157.
[15] S. Wang, W.J. Oldham Jr., R.A. Hudack, G.C. Bazan, J. Am. Chem. Soc. 122 (2000) 5695.

[16] L.-H. Chan, R.-H. Lee, C.-F. Hsieh, H.-C. Yeh, C.-T. Chen, J. Am. Chem. Soc. 124 (2001) 6469.
[17] W.J. Oldham Jr., R.J. Lachicotte, G.C. Bazan, J. Am. Chem. Soc. 120 (1998) 2987.
[18] W.-S. Han, H.-J. Son, K.-R. Wee, K.-T. Min, S. Kwon, I.-H. Suh, S.-H. Choi, D.H. Jung, S.O. Kang, J. Phys. Chem. C 113 (2009) 19686.
[19] Y.-Y. Lyu, J. Kwak, W.S. Jeon, Y. Byun, H.S. Lee, D. Kim, C. Lee, K. Char, Adv. Funct. Mater. 19 (2009) 420.
[20] Y.-Y. Lyu, J. Kwak, O. Kwon, S.-H. Lee, D. Kim, C. Lee, K. Char, Adv. Mater. 20 (2008) 2720.
[21] Y.-H. Kim, H.-C. Jeong, S.-H. Kim, K. Yang, S.-K. Kwon, Adv. Funct. Mater. 15 (2005) 1799.
[22] G. Huang, C. Yang, Z.T. Xu, H.H. Wu, J. Li, M. Zeller, A.D. Hunter, S.S.-Y. Chui, C.-M. Che, Chem. Mater. 21 (2009) 541.
[23] H.J. Kang, T.H. Noh, J.S. Jin, O.S. Jung, Inorg. Chem. 47 (2008) 5528.
[24] C. Rim, H. Zhang, D.Y. Son, Inorg. Chem. 47 (2008) 11993.
[25] M.M. Maye, J. Luo, I.I.S. Lim, L. Han, N.N. Kariuki, D. Rabinovich, T.B. Liu, C.J.T. Zhong, J. Am. Chem. Soc. 127 (2005) 1519.
[26] W. White, Z.M. Hudson, X.D. Feng, S. Han, Z.-H. Lub, S.N. Wang, Dalton Trans. 39 (2010) 892.
[27] C.-H. Chen, W.-S. Huang, M.-Y. Lai, W.-C. Tsao, J.T. Lin, Y.-H. Wu, T.-H. Ke, L.-Y. Chen, C.-C. Wu, Adv. Funct. Mater. 19 (2009) 2661.
[28] L. Zhao, S.B. Li, G.A. Wen, B. Peng, W. Hua, Mater. Chem. Phys. 100 (2006) 460.
[29] M.-H. Hu, G.-L. Shen, J.-X. Zhang, Y.-G. Yin, D. Li, Cryst. Growth Des. 9 (2009) 4533.
[30] G.-C. Xu, Y.-J. Ding, T. Okamura, Y.-Q. Huang, Z.-S. Bai, Q. Hua, G.-X. Liu, W.-Y. Sun, N. Ueyama, Cryst. Growth Des. 9 (2009) 395.
[31] K. Takagi, K. Sugihara, T. Isomura, J. Polym. Sci. Part A: Polym. Chem. 47 (2009) 4822.
[32] Z.J. Fang, S.M. Wang, L. Zhao, Z.X. Xu, J. Ren, X.B. Wang, Q.F. Yang, Mater. Chem. Phys. 107 (2008) 305.
[33] W. Pisula, F. Dierschke, K. Müllen, J. Mater. Chem. 16 (2006) 4058.
[34] S. Noro, S. Kitagawa, T. Akutagawa, T. Nakamura, Prog. Poly. Sci. 34 (2009) 240.
[35] H.Y. He, D. Collins, F.N. Dai, X.L. Zhao, G.Q. Zhang, H.Q. Ma, D.F. Sun, Cryst. Growth Des 10 (2009) 895.
[36] J. Fan, G.T. Yee, G.B. Wang, B.E. Hanson, Inorg. Chem. 45 (2006) 599.
[37] D.X. Wang, H.Y. He, X.H. Chen, S.Y. Feng, Y.Z. Niu, D.F. Sun, CrystEngComm 12 (2010) 1041.
[38] R.P. Davies, R.J. Less, P.D. Lickiss, K. Robertson, A.J.P. White, Inorg. Chem. 47 (2008) 9958.
[39] G. Kwak, T. Masuda, Macromolecules 35 (2002) 4138.
[40] J. Ohshita, T. Watanabe, D. Kanaya, H. Ohsaki, M. Ishikawa, Organometallics 13 (1994) 5002.
[41] H. Zhang, Q. Cai, D.W. Ma, J. Org. Chem. 70 (2005) 5164.
[42] P.M. Beaujuge, J.R. Reynolds, Chem. Rev. 110 (2010) 268.
[43] Z.Q. Jiang, H.Q. Yao, Z.Y. Liu, C.L. Yang, C. Zhong, J.G. Qin, G. Yu, Y.Q. Liu, Org. Lett. 11 (2009) 4132.
[44] Y.-L. Liu, X.-Q. Ran, J.-K. Feng, A.-M. Ren, L.-Y. Zou, Aust. J. Chem. 63 (2010) 125.
[45] M.J. Frisch, G.W. Trucks, H.B. Schlegel, G.E. Scuseria, M.A. Robb, J.R. Cheeseman, J.A. Montgomery Jr., T. Vreven, K.N. Kudin, J.C. Burant, J.M. Millam, S.S. Iyengar, J. Tomasi, V. Barone, B. Mennucci, M. Cossi, G. Scalmani, N. Rega, G.A. Petersson, H. Nakatsuji, M. Hada, M. Ehara, K. Toyota, R. Fukuda, J. Hasegawa, M. Ishida, T. Nakajima, Y. Honda, O. Kitao, H. Nakai, M. Klene, X. Li, J.E. Knox, H.P. Hratchian, J.B. Cross, C. Adamo, J. Jaramillo, R. Gomperts, R.E. Stratmann, O. Yazyev, A.J. Austin, R. Cammi, C. Pomelli, J.W. Ochterski, P.Y. Ayala, K. Morokuma, G.A. Voth, P. Salvador, J.J. Dannenberg, V.G. Zakrzewski, S. Dapprich, A.D. Daniels, M.C. Strain, O. Farkas, D.K. Malick, A.D. Rabuck, K. Raghavachari, J.B. Foresman, J.V. Ortiz, Q. Cui, A.G. Baboul, S. Clifford, J. Cioslowski, B.B. Stefanov, G. Liu, A. Liashenko, P. Piskorz, I. Komaromi, R.L. Martin, D.J. Fox, T. Keith, M.A. Al-Laham, C.Y. Peng, A. Nanayakkara, M. Challacombe, P.M.W. Gill, B. Johnson, W. Chen, M.W. Wong, C. Gonzalez, J.A. Pople, Gaussian 03, Revision B.04. Gaussian, Inc., Pittsburgh, PA), 2003.
[46] A.P. Kulkarni, C.J. Tonzola, A. Babel, S.A. Jenekhe, Chem. Mater. 16 (2004) 4556.
[47] H.-H. Wang, L. Xue, Y.-Y. Qian, H. Jiang, Org. Lett. 12 (2010) 292.
[48] A. Chatterjee, M. Santra, N. Won, S. Kim, K.J. Kim, B.S. Kim, H.K. Ahn, J. Am. Chem. Soc. 131 (2009) 2040.
[49] L. Liu, D. Zhang, G. Zhang, J. Xiang, D. Zhu, Org. Lett. 10 (2008) 2271.
[50] S.R. Meech, D.C. Philips, J. Photochem. 65 (1983) 229.
[51] J.P. Cross, M. Lauz, P.D. Badger, S. Petoud, J. Am. Chem. Soc. 126 (2004) 16278.